THE JOURNAL OF BIOLOGICAL CHEMISTRY
Vol. 279, No. 40, Issue of October 1, pp. 42250–42257, 2004

Printed in U.S.A.

Tryptophan Scanning Mutagenesis of the γM4 Transmembrane Domain of the Acetylcholine Receptor from *Torpedo californica**

Received for publication, May 10, 2004, and in revised form, June 21, 2004
Published, JBC Papers in Press, July 9, 2004, DOI 10.1074/jbc.M405132200

Alejandro Ortiz-Acevedo‡§, Mariel Melendez‡¶, Aloysha M. Asseo‡, Nilza Biaggi‡, Legier V. Rojas‖, and José A. Lasalde-Dominicci‡**

From the ‡University of Puerto Rico, Department of Biology, San Juan, Puerto Rico 00931-3360 and the ‖Universidad Central del Caribe, School of Medicine, Department of Physiology, Bayamon, Puerto Rico 00960-6032

The periodicity of structural and functional effects induced by tryptophan scanning mutagenesis has been successfully used to define function and secondary structure of various transmembrane domains of the acetylcholine receptor of *Torpedo californica*. We expand the tryptophan scanning of the AchR of *T. californica* to the γM4 transmembrane domain (γTM4) by introducing tryptophan, at residues 451–462, along the γTM4. Wild type (WT) and mutant AChR were expressed in *Xenopus laevis* oocytes. Using [^{125}I]α-bungarotoxin binding assays and voltage clamp, we determined that the nAChR expression, EC_{50}, and Hill coefficient values for WT are 1.8 ± 0.4 fmol, 30.3 ± 1.1 μM, and 1.8 ± 0.3, respectively. Mutations L456W, F459W, and G462W induce a significant increase in nAChR expression (2.8 ± 0.5, 3.6 ± 0.6, and 3.0 ± 0.5 fmol, respectively) when compared with WT. These data suggest that these residues are important for AChR oligomerization. Mutations A455W, L456W, F459W, and G462W result in a significant decrease in EC_{50} (19.5 ± 1.7, 11.4 ± 0.7, 16.4 ± 3.8, and 19.1 ± 2.6 μM, respectively), thus suggesting a gain in function when compared with WT. In contrast, mutation L458W induced an increase in EC_{50} (42.8 ± 6.8 μM) or loss in function when compared with WT. The Hill coefficient values were the same for WT and all of the mutations studied. The periodicity in function (EC_{50} and macroscopic peak current) and nAChR expression reveals an average of 3.3 and 3.0 amino acids respectively, thus suggesting a helical secondary structure for the γTM4.

The nicotinic acetylcholine receptor (AChR)[1] from *Torpedo californica* belongs to a family of ligand-gated ion channels that include the serotonin 5-hydroxytryptamine type 3, γ-aminobutyric acid, and glycine receptors (for review see Refs. 1 and 2). The AChR is an allosteric, integral membrane protein comprised of five subunits arranged pseudo-symmetrically with a $\alpha_2\delta\gamma\beta$ stoichiometry (3, 4). The five subunits cross the membrane and form a ring around the ion channel in the center. Each subunit consists of a large hydrophilic N terminus, four transmembrane domains (TM) of 20–30 amino acids denoted M1–M4 (see Fig. 1), an intracellular loop between M3 and M4, and a short extracellular C terminus (5). The M2 transmembrane domain (TM2) from each subunit lines the channel pore in the closed state conformation, whereas TM1 and TM2 contribute to the formation of the ion channel pore in the open state of the AChR (6). TM3 and TM4 segments are, however, in contact with membrane lipids, and photolabeling techniques have been used to identify the lipid-exposed residues of all of the AChR subunits (7, 8).

A high resolution structure from a crystallized AChR has not been reported yet; however, a recent cryomicroscopy study of the AChR structure has achieved resolutions down to 4 Å (9). Consequently, the model proposed in the latter study has become the best approximation to the AChR structure. Other alternative approaches to crystallization have been utilized to probe both AChR structure and function. Examples of these techniques include Fourier transformed infrared spectroscopy (10–12), photoaffinity labeling (7, 8), and two-dimensional ^{1}H-NMR spectroscopy (13). A variation of site-directed mutagenesis, tryptophan scanning mutagenesis, has also been successfully used to characterize transmembrane domains of proteins like the Na/K-ATPase (14) and the γ-aminobutyric acid, type A receptor (15, 16).

Tryptophan scanning and/or site-directed mutagenesis have been used to gather valuable data about the structure and function of various transmembrane domains of the AChR, with emphasis on the lipid-exposed residues (17–24). For example, site-directed mutagenesis was used to replace the lipid-exposed residues αCys^{418} and αCys^{421} (7, 8) with tryptophan (19, 20). These mutations resulted in a substantial increase in channel open time and demonstrated the important role of these residues in the AChR channel gating. Tryptophan scanning of several TM domains of the AChR has been successfully used to assess the structure and function of the AChR. This approach has been used for the αTM4 (17), γTM3 (25), αTM3 (26), and βTM3 (27) subunits of the AChR. The results from these studies have identified residues at which a tryptophan replacement results in a robust gain in function. Some examples of these sites are αCys^{418} (19), αVal^{425} (17), βCys^{447} (20), γLeu^{296} (25), and αThr^{422} (24). Moreover, analysis of the changes in AChR function and expression as a function of the mutation position or periodicity has given valuable information used to predict the secondary structure of various transmembrane domains of the AChR. The periodicity for αTM3-TM4 and βTM3 are all consistent with a helical structure for these transmembrane domains (17, 26, 27).

In this study, we extend the tryptophan scanning mutagenesis to the γTM4 transmembrane domain of the AChR from *T. californica*. The purpose of this study is to determine the role of

* This work was supported by NIGMS, National Institutes of Health Grants GM56371-05 and GM08102-27. The costs of publication of this article were defrayed in part by the payment of page charges. This article must therefore be hereby marked "*advertisement*" in accordance with 18 U.S.C. Section 1734 solely to indicate this fact.
§ Supported by a Postdoctoral Supplement to Grant GMRO156371.
¶ Supported by Minority Access to Research Careers-National Institutes of Health Grant 5T34GM07821 and the SCORE Program.
** To whom correspondence should be addressed: University of Puerto Rico, Dept. of Biology, San Juan, PR 00931. Tel.: 787-764-0000 (ext. 2765/4887); Fax: 787-753-3852; E-mail: joseal@coqui.net.
[1] The abbreviations used are: AChR, acetylcholine receptor; ACh, acetylcholine; TM, transmembrane domain; WT, wild type; BTX, bungarotoxin.

the γTM4 transmembrane domain on the AChR function and to use the data gathered to make predictions about the secondary structure of γTM4. Eleven residues in the middle of γTM4, Cys^{451}–Gly^{462}, were selected for this study. Two of these residues, Cys^{451} and Ser^{460}, have been reported to be exposed to the membrane lipids (7, 8). We expressed WT and mutated AChRs in *Xenopus* oocytes. The nAChR expression was determined using [^{125}I]α-BTX binding assays, and functional studies were performed using two electrode voltage clamp to determine ACh-induced currents. We found that mutations L456W, F459W, and G462W resulted in a significant increase in nAChR expression when compared with that of WT. The rest of the mutations showed nAChR expression levels similar to WT. All of the mutations that increased nAChR expression and A455W produced an increase in function, as evidenced by a decrease in EC_{50} relative to WT. Seven mutations, I454W, A455W, L456W, L457W, F459W, I461W, and G462W resulted in an increase in macroscopic response (I_{max}) relative to WT. Mutations I454W, A455W, L457W, and L458W caused a significant increase in the normalized macroscopic response (I_{max}/fmol) induced by ACh. The average periodicity calculated for nAChR expression, EC_{50}, and I_{max} suggest a helical secondary structure for γTM4.

EXPERIMENTAL PROCEDURES

Mutations in the γTM4 Transmembrane Domain—A QuikChange site-directed mutagenesis kit (Stratagene, La Jolla, CA) was used to replace the existing amino acids with tryptophan, at positions 451–462 of the γ subunit of the AChR. The PCR product was used to transform *Epicurian coli* XL1 supercompetent cells. The DNA was then purified using a QIAprep spin miniprep kit (Qiagen) and sequenced to ensure a successful mutation.

nAChR Expression in Xenopus laevis Oocytes—mRNA transcripts were synthesized *in vitro*. The mRNA transcripts for α, β, γ, and δ subunits were microinjected into *X. laevis* oocytes at a 2:2:1:1 ratio. The volume of mRNA mix injected was varied depending upon the concentration of the mRNA mix.

Voltage Clamp on Xenopus Oocytes—ACh-induced currents were recorded 3 days after mRNA microinjection using a two-electrode voltage clamp. The electrodes were filled with 3 M KCl (resistance, <2 MΩ). Impaled oocytes were perfused at a rate of 0.5 ml/s with MOR-2 buffer (82 mM NaCl, 2.5 mM KCl, 5 mM $MgCl_2$, 1 mM Na_2HPO_4, 5 mM HEPES, and 0.2 mM $CaCl_2$, pH 7.4). The membrane potential of each oocyte was clamped at −70 mV during the experiment. The membrane currents were digitized and filtered at 2 kHz using an Axon DigiData interface (Axon Instruments) and recorded using the Whole Cell Analysis Program, version 3.2.9 (provided by John Dempster, University of Strathclyde, UK). This program is installed on a Pentium III-based computer. Dose-response data were collected from peak currents (*I*) observed for each of the six ACh concentrations used (1, 3, 10, 30, 100, and 300 μM). The GraphPad Prism software (GraphPad Software Incorporated, San Diego, CA) was used to perform a nonlinear regression fit with a sigmoidal dose-response (variable slope) equation,

$$I = I_{min} + (I_{max} - I_{min}/1 + 10^{(LogEC_{50} - Log[ACh]) \times Hill\ Slope}) \quad \text{(Eq. 1)}$$

where *I* is the macroscopic current at a given ACh concentration, I_{min} and I_{max} are the smallest and the largest current observed, respectively, EC_{50} is the concentration required to achieve half-maximal response, and the Hill Slope is the slope of the linear portion of the sigmoidal curve.

[^{125}I]α-Bungarotoxin Binding Assay—We performed [^{125}I]α-bungarotoxin (Amersham Biosciences) binding assays to determine the membrane expression of AChR in oocytes. The oocytes were incubated in 10 nM [^{125}I]α-bungarotoxin with 5 mg/ml albumin serum bovine in MOR-2 without EGTA at room temperature for 1.5 h. Noninjected oocytes were also incubated in [^{125}I]α-bungarotoxin to measure nonspecific binding (Beckman Gamma 5500). Excess toxin was removed by washing each oocyte with 15 ml of MOR-2 without EGTA. A standard curve was obtained by plotting the counts/min against [^{125}I]α-bungarotoxin concentration (0.5–20 fmol). The equation for the linear regression obtained from this graph of counts/min *versus* volume (μl) was used to calculate the AChR expression (fmol) present in the membrane of each oocyte. The nAChR expression was determined for two groups of oocytes. One of these groups consists of oocytes used in the dose-response experiments, whereas the other group of oocytes belonged to experiments performed solely to calculate nAChR expression as a function of mutation. The nAChR expression value for the first group of oocytes was used to calculate the normalized channel response to ACh for each mutation, which is defined as the ACh-induced current in nanoamperes divided by femtomole of surface α-bungarotoxin binding. The expression calculated for the second group of oocytes was used to plot nAChR expression as a function of mutation along the γTM4 domain.

Statistical Analysis—We compared nAChR expression level (fmol), EC_{50}, Hill coefficient, and maximal current values between wild type and each mutation. The data were analyzed using the SPSS general linear model procedure for one-way analysis of variance to perform planned comparisons between these groups.

Calculation of Periodicity for Both nAChR Expression and EC_{50}—The expression of each mutant was normalized to the change in amino acid volume (Å^3) caused by each tryptophan substitution. Tryptophan being the largest amino acid, this change corresponds to the volume of tryptophan (Å^3) minus the volume of the WT amino acid replaced with tryptophan. The amino acid volumes used in this study were obtained from the calculations of Chothia (28). We then constructed plots of the normalized nAChR expression values as a function of their position along the γTM4 domain. Separate plots were created using EC_{50} and macroscopic response (I_{max}) values, for both WT and mutants, as a function of residue in the γTM4 domain. A cubic spline function (GraphPad Software Incorporated, San Diego, CA) was found to best fit the fluctuations induced by the tryptophan replacements, in normalized nAChR expression, EC_{50}, and I_{max} data. To calculate the periodicity, we first determined the amino acid positions in which the first derivative of the cubic spline function is zero and then calculated the distance between the zeros.

Topological Representation of the γTM4—The structural model for the γ subunit presented in Fig. 6 corresponds to that proposed by Miyazawa *et al.* (9). This structure was downloaded from the NCBI Structure data base (www.ncbi.nlm.nih.gov/entrez/query.fcgi?CMD=search&DB=structure). The structure was then exported to DS ViewerPro 5.0 (Accelrys; www.accelrys.com) and edited for publication.

RESULTS

nAChR Expression of γTM4 Mutants—Tryptophan scanning mutagenesis was performed on the γTM4 of *Torpedo* AChR, from residues Cys^{451}–Gly^{462} (Fig. 1), as explained under "Experimental Procedures." Subsequently, *Xenopus* oocytes were injected with mRNA encoding the mutated γ subunit and the wild type α, β, and δ subunits. [^{125}I]α-BTX binding assays were performed 3 days after injection to determine the effect of each mutation on the nAChR expression level of AChR. The results of these binding assays are summarized in Fig. 2. The average WT expression was 1.8 ± 0.4 fmol (Fig. 2). Three of the mutations studied, L456W, F459W, and G462W exhibited nAChR expression levels significantly higher than that of WT. Specifically, L456, F459W, and G462W resulted in 1.6-, 2.0-, and 1.7-fold increases in nAChR expression, respectively (Fig. 2). The rest of the mutations resulted in expression levels similar to that of WT, thus suggesting that the secondary structure of γTM4 is loose enough to accommodate a large hydrophobic amino acid, such as tryptophan, without major consequences to the AChR assembly. Moreover, the increase in nAChR expression detected for three of the mutants suggests that, at those positions, tryptophan facilitates the AChR assembly and/or oligomerization. The tryptophan scanning results obtained with γTM4 are in contrast with those found with αTM4 (17), αTM3 (26), and βTM3 (27), in which 23 of a total of 40 mutations examined either prevented or markedly decreased the expression of the AChR. Moreover, from these 40 mutations, only αI286W and βM285W resulted in a significant increase in nAChR expression when compared with WT (26, 27).

Functional Effects of γM4 Trp Scanning of the AChR; ACh-induced Currents—The TM4 domain is the most lipophilic of all of the subunits of the AchR, and some of the residues in this TM domain are known to be exposed to the membrane lipids (7, 8). The purpose of these studies is to determine the role of γTM4

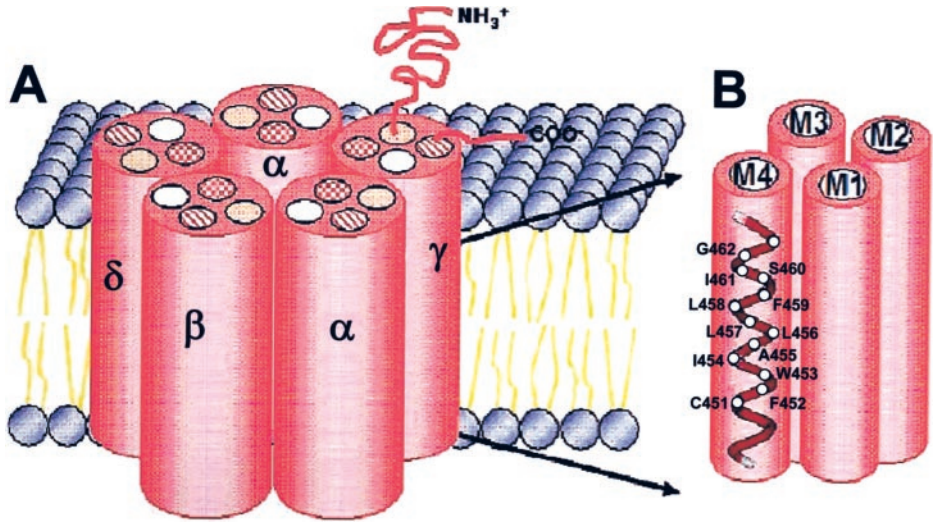

FIG. 1. **Topological representation of the AChR.** *Left panel*, diagram of the AChR pentamer. *Right panel*, illustration of the tryptophan scanning mutagenesis performed on the γTM4 transmembrane domain. The WT amino acid was replaced with tryptophan at residues Cys^{451}–Gly^{462}.

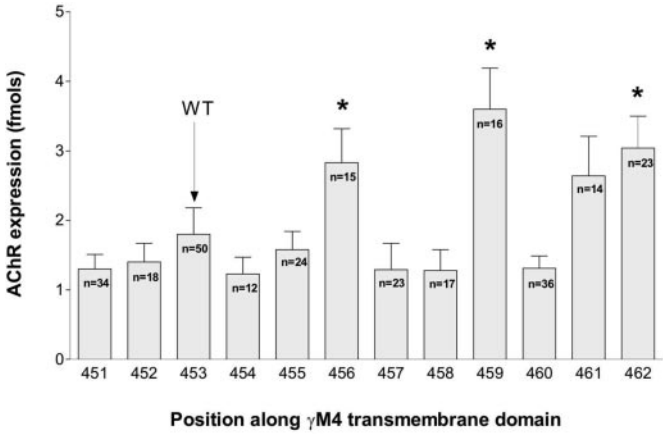

FIG. 2. **Expression of wild type and mutant AChRs.** [^{125}I]α-BTX binding assays were performed to determine the nAChR expression level of each group of oocytes. The *bars* represent the average level of nAChR expression (fmol) ± S.E. Each *bar* includes the number of oocytes used to calculate the nAChR expression average. The *asterisks* represent nAChR expression averages that are significantly different from that of wild type ($p < 0.01$).

on channel function and to assess the role that lipid-protein interactions may have on the AChR function. We used the two electrode voltage clamp technique to determine the dose response for ACh, using ACh concentrations ranging from 1 to 300 μM. Fig. 3 illustrates representative current traces induced by the different ACh concentrations used for both mutants and WT. All of the mutations studied yielded functional AchRs, and some mutations (*e.g.* I454W, A455W, and L456W) resulted in a gain in function (Fig. 3). Table I contains the average maximal current (I_{max}) or current induced by 300 μM for each oocyte. Mutations I454W, A455W, L456W, L457W, F459W, I461W, and G462W resulted in macroscopic response (I_{max}) values significantly higher than that of WT, with *n*-fold values ranging from 2.3–3.4-fold. When the I_{max} values were normalized to the nAChR expression level (fmol) for each oocyte (normalized macroscopic response), mutations I454W, A455W, L457W, and F458W were found to display normalized currents significantly higher than WT, with *n*-fold increase values of 3.4-, 10.7-, 7.0-, and 4.5-fold, respectively. No mutation resulted in a decrease of either I_{max} of I_{max}/fmol. These results contrast our previously reported findings with αTM4 (17), αTM3 (26), and βTM3 (27). In those studies, 21 of a total of 40 mutations studied resulted in a decrease in I_{max}, and five mutations resulted in nonfunctional receptors. In contrast, eight of the total of 40 mutations examined in αTM4 (17), αTM3 (26), and βTM3 (27) resulted in normalized currents higher than the controls (WT).

We used the dose-response data (Fig. 4) to calculate the EC_{50} for ACh and the AChR Hill coefficient for each mutation. The average for the EC_{50}, Hill coefficients, and I_{max} for each condition are presented in Table I. Four mutations, A455W, L456W, F459W, and G462W, resulted in a significant decrease in EC_{50} (*i.e.* gain in function), when compared with WT. In contrast, one mutation, L458W, resulted in an increase in EC_{50}, thus demonstrating a loss in function as a result of a tryptophan substitution at that position. There was no significant difference between the Hill coefficient values of WT and mutants.

DISCUSSION

Overview—The purpose of this study was to determine the role of the γTM4 transmembrane domain on the AChR function. To that end, we performed tryptophan scanning mutagenesis on 11 residues, Cys^{451}–Gly^{462}, of the γTM4 transmembrane domain from the AChR of *T. californica*. Results from independent studies (7, 8) suggest that two of these residues, Cys^{451} and Ser^{460}, are exposed to membrane lipids. The AChR receptor was expressed in *Xenopus* oocytes and the effect of each tryptophan substitution on nAChR expression and channel function was assessed. Receptor expression was determined with [^{125}I]α-BTX binding assays, whereas functional studies were performed using two electrode voltage clamp to determine ACh-induced currents for both WT and mutants.

We found that mutations L456W, F459W, and G462W resulted in a significant increase in nAChR expression when compared with that of WT. The rest of the mutations showed nAChR expression levels similar to WT. All of the mutations that caused increased nAChR expression and mutation A455W produced an increase in function, as evidenced by a decrease in EC_{50} relative to WT. Seven mutations, I454W, A455W, L456W, L457W, F459W, I461W, and G462W, resulted in an increase in macroscopic response (I_{max}) relative to WT. Mutations I454W, A455W, L457W, and L458W caused a significant increase in the normalized macroscopic response (I_{max}/fmol) induced by ACh. An analysis of the functional and structural implications of these results follows.

Expression of AChRs with Mutations on γTM4—Our results demonstrate that the introduction of tryptophan, the largest and most lipophilic amino acid, did not result in a decrease in nAChR expression in any of the mutants studied. Moreover, three of the mutations studied, L456W, F459W, and G462W, resulted in significant 1.6–2-fold increase in nAChR expression relative to WT (Fig. 2). These results differ markedly from

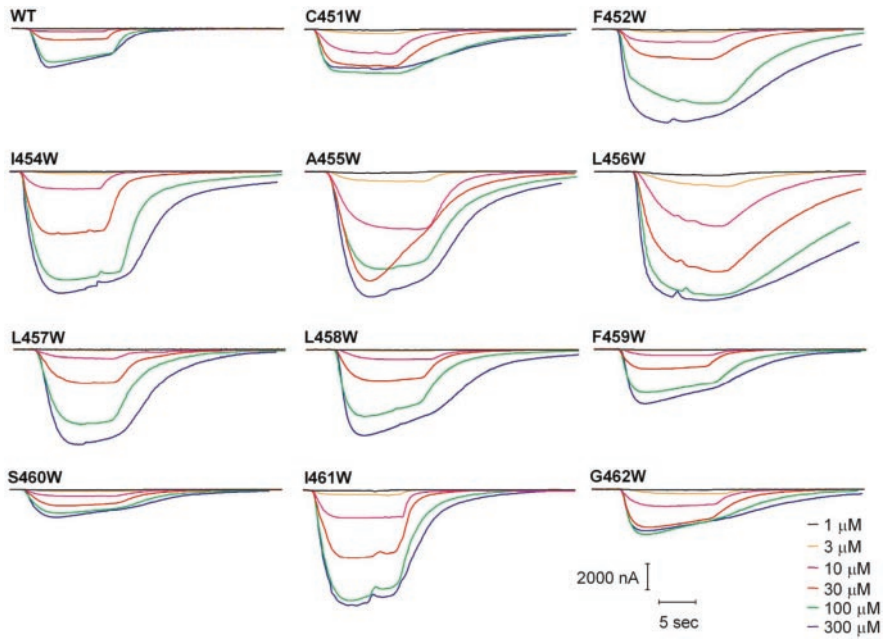

FIG. 3. **Macroscopic currents as a function of acetylcholine concentration.** This figure illustrates representative traces of ACh-induced macroscopic currents for both WT and the γTM4 mutants studied. The acetylcholine concentrations used range from 1 to 300 μM.

TABLE I
Functional parameters of wild type and γTM4 mutants

Comparison of the functional parameters of wild type and all the γTM4 mutants generated in this study. The values are given as the means ± S.E.

nAChR type	EC_{50}	Hill coefficient	I_{max}	I_{max}	*n*
	μM		*nA/fmol*	*nA*	
WT	30.29 ± 1.06	1.75 ± 0.32	3889 ± 996	3287 ± 659	35
C451W	28.49 ± 2.23	1.53 ± 0.07	2803 ± 674	3706 ± 926	26
F452W	28.03 ± 3.73	1.46 ± 0.07	5043 ± 1059	6294 ± 572	12
I454W	36.67 ± 5.38	1.32 ± 0.08	13270 ± 2024[a]	9821 ± 1157[a]	8
A455W	19.48 ± 1.69[b]	1.29 ± 0.08	41441 ± 11610[b]	11019 ± 1058[b]	16
L456W	11.38 ± 0.72[b]	1.41 ± 0.09	4387 ± 888	10904 ± 1157[b]	9
L457W	34.61 ± 3.89	1.26 ± 0.09	26759 ± 15147[b]	7603 ± 1049[a]	14
L458W	42.79 ± 6.77[a]	1.40 ± 0.08	17438 ± 8076[a]	5809 ± 1136	9
F459W	16.40 ± 3.77[b]	1.38 ± 0.09	2967 ± 306	9799 ± 1605[b]	10
S460W	30.27 ± 1.71	1.37 ± 0.07	2866 ± 938	2106 ± 404	29
I461W	28.93 ± 3.98	1.69 ± 0.08	3601 ± 566	8322 ± 2224[a]	8
G462W	19.10 ± 2.59[b]	1.45 ± 0.06	5535 ± 1228	6533 ± 1017[a]	17

[a] $p < 0.01$.
[b] $p < 0.0001$.

those found in αTM4 (17), αTM3 (26), and βTM3 (27) from *T. californica*. Taken together, these three studies evaluated the effect of a total of 40 tryptophan replacements at different residues of each of the TM domains. From these, 23 such replacements resulted in either prevention or a marked decrease in nAChR expression when compared with WT and only two mutations, αI286W and βM285W, resulted in an increase in nAChR expression (26, 27). The results obtained with αTM3, αTM4, and βTM3 thus demonstrate that the steric hindrance caused by the introduction of a large amino acid drastically decreases the efficiency of receptor assembly and suggest that these subunits are more tightly packed than γTM4. Consequently, it is possible that γTM4 has a larger membrane crossing angle than α and β subunits, thereby allowing the introduction of a tryptophan residue without major consequences to the AChR assembly. We thus hypothesize that the high tolerance for tryptophan replacements exhibited by γTM4 is the result of a loosely packed arrangement of its residues and/or a wide crossing angle in the membrane.

In contrast to the results obtained with α and β subunits, the results presented in this study are consistent with those reported for γTM3 from *T. californica* (25). In this study, a total of eight tryptophan substitutions were performed in this transmembrane domain, and all of the mutations resulted in nAChR expression levels similar to WT. These results demonstrate that γTM3 and γTM4 can accommodate the introduction of tryptophan without major consequences to the efficiency of nAChR assembly. Moreover, in the case of γTM4, introducing tryptophan at three residues (L456W, F459W, and G462W) increased the expression of the AChR and thus suggests that, at these positions, a large and lipophilic amino acid facilitates receptor assembly. The results obtained with αTM3-TM4, βTM3, and γTM3-TM4 are all consistent with the hypothesis that the transmembrane segments of the γ subunit are less tightly packed toward the interior of the AChR and/or have a wider crossing angle than α or β subunits.

Functional Correlations—The functional parameters calculated for the L456W, F459W, and G462W reveal a notable finding. These three mutations resulted in increased nAChR expression and displayed a gain in function when compared with WT, as evidenced by their lower EC_{50} and increased macroscopic response (I_{max}) values (Table I). Of the aforementioned mutations, L456W results in the highest gain in function and a 3.3-fold increased macroscopic response. These results suggest that, at these residues, the increased efficiency in channel assembly induced by tryptophan replacement also lead to a stabilization of the open state of AChR and consequently a gain in channel function. Moreover, these results suggest that

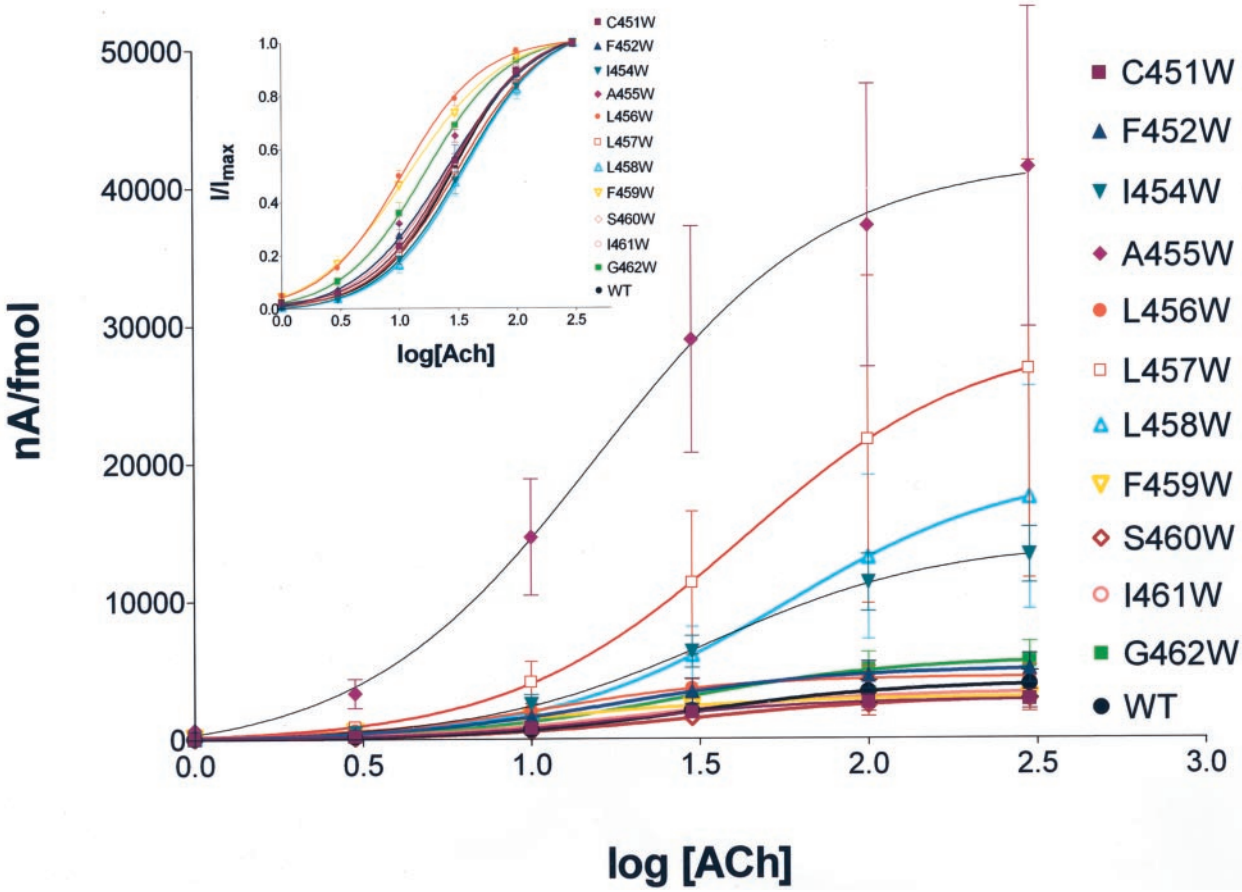

FIG. 4. **Dose-response curves for acetylcholine for WT and γTM4 mutants.** The maximum current induced by each acetylcholine concentration (*I*) was determined and normalized for the nAChR expression (fmol) of each oocyte. The data are thus presented as nA/fmol as a function of log[ACh]. In addition, each current was normalized to the current induced by the highest acetylcholine concentration (*i.e.* 300 μM; I_{max}). The latter is presented in the *inset* as I/I_{max} as a function of log[ACh]. The sigmoidal curves thus generated were used to calculate both the EC_{50} and Hill Slope for acetylcholine (Table I).

these three residues play an important role in AChR gating.

Four additional mutations, I454W A455W, L457W, and L458W resulted in a significant increase in channel function and/or macroscopic response. L457W and I454W resulted in no change in EC_{50} but displayed a significant increase in both macroscopic and normalized macroscopic responses. The most dramatic increase in response was detected for mutation A455W, which resulted in a significant decrease in EC_{50} ($p < 0.0001$), a 3-fold increase in macroscopic response, and an 11-fold increase in normalized macroscopic response. These results suggest that introducing tryptophan at residue Ala^{455} results in the stabilization of the open channel conformation of the AChR, and therefore this position plays an important role in the AChR gating. The macroscopic responses detected in mutations A455W, L457W, and L458W constitute the largest observed of all of the tryptophan substitutions that we have reported so far. Future single-channel characterization of these mutants will provide important information necessary to understand the mechanism of action of tryptophan at these positions.

The L458W is the only mutation that displayed a significant increase in EC_{50} from all of the γTM4 mutants examined in the present study. According to a previous photolabeling study (8), position Leu^{458} is facing toward the interior of the protein. Moreover, a recent AChR structure model (9) places this position facing the γTM1 domain (see Fig. 6). The moderate increase in EC_{50} observed for the L458W mutation is the only indication of a possible inhibitory effect; however, the normalized current was significantly larger than that of WT. Furthermore, the nAChR expression level of this mutant is not significantly different from that of WT. These data indicate that the volume increase at this position does not affect nAChR assembly yet results in a minor increase in EC_{50}.

The functional data obtained for γTM4 differs noticeably from that obtained for αTM4 (17), αM3 (26), and βTM3 (27) for *T. californica*. Taken together, these studies found that in 83% of the cases, a tryptophan replacement at these TM domains results in a decrease in either macroscopic or normalized macroscopic responses. In fact, tryptophan replacement in residues like αI417W (17), αM282W (26), and βI296W (27) resulted in a complete loss of AChR assembly. Finally, the results for γTM4 are consistent with those obtained with γTM3, in which only one of seven tryptophan substitutions resulted in a decreased normalized macroscopic response, whereas 43% of the mutations resulted in an increase in normalized macroscopic response (25). These functional results are consistent with the trend seen with the nAChR expression data (see above), in that they demonstrate that tryptophan replacements in both α and β subunits result in a decrease in function, whereas in the γ subunit these substitutions result in either an increase or no change in function, relative to WT.

Structural Interpretation—Even though a high resolution structure from a crystallized AChR has not been reported yet, several research groups have used various alternative approaches in an effort to gain insight on the secondary structure of the TM domains of the AChR. Hydrophobicity plots of the transmembrane domains of the AChR from *T. californica* suggest that the secondary structure for these domains is an α-he-

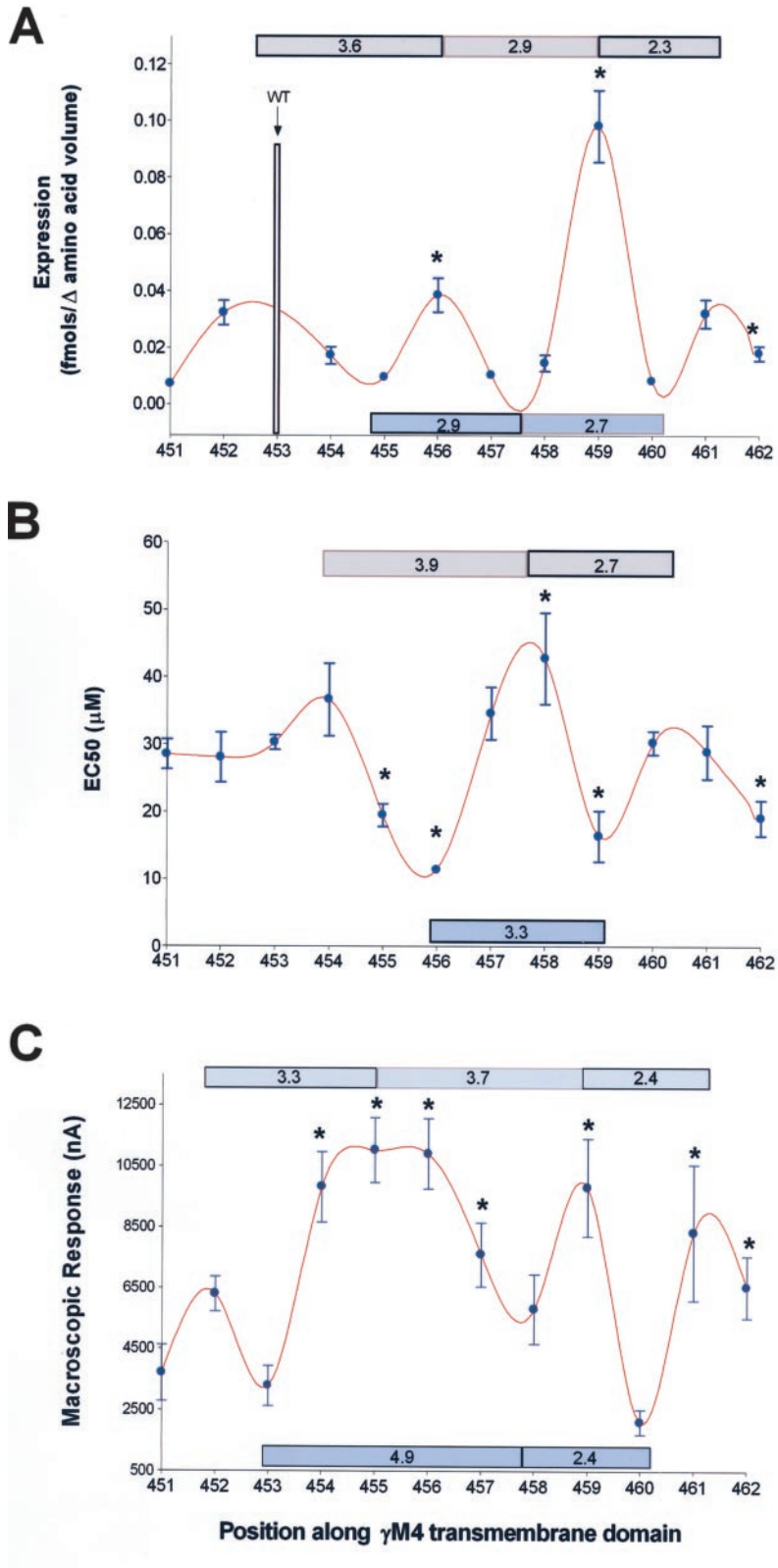

FIG. 5. **Periodicity of changes in AChR-normalized nAChR expression and function plotted as a function of residue position along the γTM4 transmembrane domain.** *A*, plot for normalized nAChR expression levels (femtomoles of AChR expressed by each mutant divided by the difference in amino acid volume of the original residue and tryptophan). *B*, EC_{50} values for both wild type and mutants illustrate the functional effects of each mutation. *C*, macroscopic response (I_{max}) for wild type and mutants demonstrating the functional effect of each mutation. The *asterisks* represent parameters that are significantly different from those calculated for WT (see Table I for details).

lix (29, 30). Studies utilizing Fourier transformed infrared spectroscopy also arrived to a similar conclusion about the TM domains of the AChR from *T. californica* (11, 12, 31). Photoaffinity labeling studies conducted to delineate the lipid-exposed residues of different TM domains from *T. californica* indicate that the labeling pattern for various TM domains is consistent with that of an α helix (7, 8). Data from two-dimensional ^1H NMR spectroscopy studies also suggest a helical structure for a synthetic peptide of αTM3 from *T. californica* (13). Finally, cryomicroscopy has been used in an effort to elucidate the structure of the AChR from *Torpedo marmorata* (32, 33). In one of the initial cryomicroscopy reports, a structure at 9-Å resolution was reported and led the author to conclude that only the TM2 domains lining the pore are α-helical, whereas TM1, TM3,

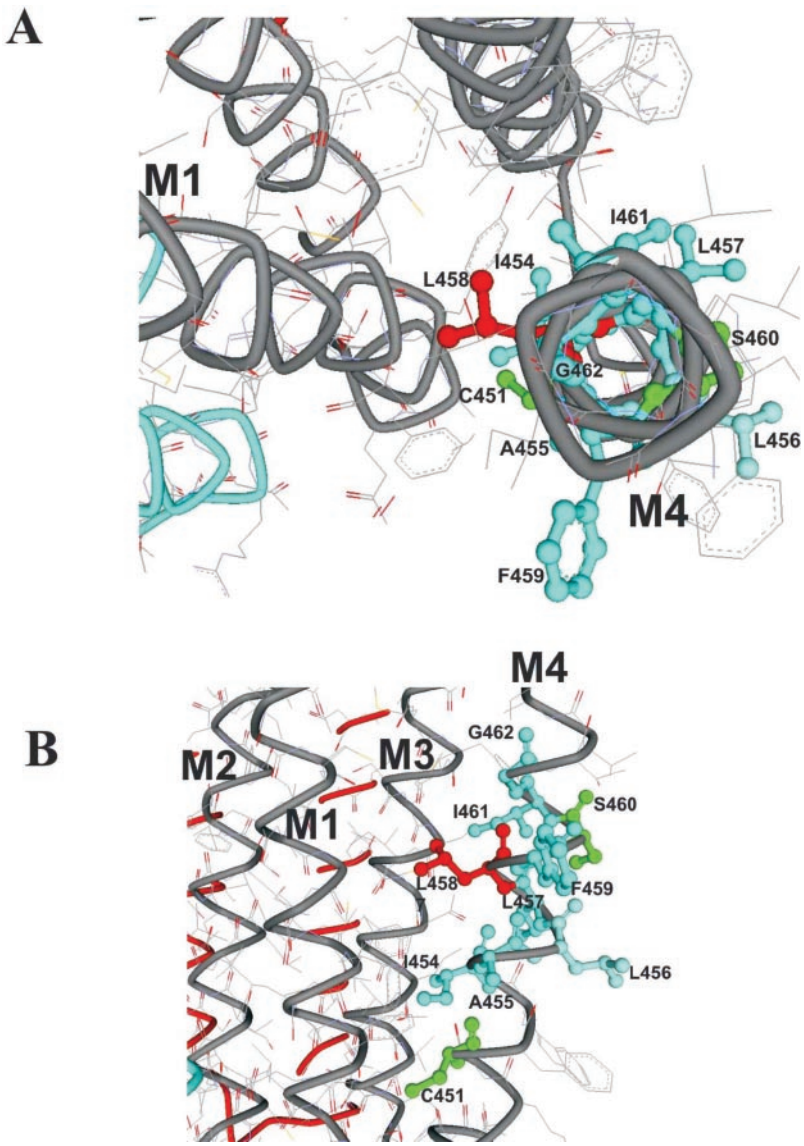

FIG. 6. **nAChR expression and functional data illustrated using the γ subunit model proposed by Miyazawa *et al.* (9).** TM domains 1–4 of the γ subunit are displayed as *gray* α-helices and marked as *M1–M4*. Cys^{451} and Ser^{460} (*green*) have been proposed to be lipid-exposed (8). Tryptophan replacement at residue Leu^{458} (*red*) resulted in a moderate increase in EC_{50}. An increase in nAChR expression, decreased EC_{50}, and increased macroscopic response were detected when tryptophan was introduced in residues Leu^{456}, Phe^{459}, and Gly^{462} (*blue*). Tryptophan replacement in residues Ile^{454}, Ala^{455}, Leu^{457}, and Ile^{461} (*blue*) resulted in increased macroscopic and/or normalized macroscopic response. *A*, view from top of γTM4. *B*, side view of γTM4.

and TM4 are β-sheets (34). A recent study from the same research group (9) concludes that the secondary structure of all of the transmembrane domains of the AChR is α-helical, yet no explanation is given for such a fundamental change in their model.

Another approach that has proven useful to predict protein structural patterns, as they relate to function, is tryptophan scanning mutagenesis. This approach has been used to characterize transmembrane segments from several proteins. These include the MotA proton channel (35, 36), the α_2TM2 and α_1TM4 transmembrane domains of the γ-aminobutyric acid, type A receptor (15, 16), and the Na/K-ATPase (14). Our laboratory has used this approach to predict structural patterns of transmembrane domains from various subunits of the AChR like αTM4 (17), γTM3 (25), αTM3 (26), and βTM3 (27) from *T. californica*. In this study, we have performed tryptophan scanning mutagenesis along the central portion of the γTM4 transmembrane domain from *T. californica*.

The detection of the surface AChR is not dependent upon AChR activation; thus the periodicity of nAChR expression reveals structural information about the closed or resting state. In contrast, the periodicity of functional parameters reveals structural information about the open state of the channel, because EC_{50} values are determined from the peak macroscopic response, or I_{max}, induced by ACh. Fig. 5*A* illustrates the periodicity of nAChR expression for each of the tryptophan replacements studied. We have found that normalizing the nAChR expression level of each mutant to the change in amino acid volume (fmol/ΔVol) at each residue provides a better representation of the steric disruption caused by each tryptophan substitution (26) and thus an improved approximation of the degree to which the net amino acid volume change affects the expression of the AChR. We have proposed that the reason for this observation is that transmembrane segments of the AChR are tightly packed, and thus side chain volume of residues in the transmembrane domain is the most critical property for heteropentamer assembly and consequently ion channel function (26). Moreover, in the case of the γM4 positions selected for this study, there are only two polar residues (Ser^{460} and Cys^{451}), whereas the other nine residues (three leucines, two phenylalanines, two isoleucines, one alanine, and one glycine) are hydrophobic, with the exception of glycine, which is nonpolar aliphatic. Because of the homogeneous nature of the *R* groups of the amino acids in γTM4 and the tightly packed nature of transmembrane domains, it is reasonable to propose that the predominant effect of the tryptophan replacement is that caused by a net increase in amino acid side chain volume. The normalized nAChR expression data in Fig. 5*A* reveals three phases with an average periodicity of 3 amino acids for phases I, II, and III. The periodicity for the EC_{50} (Fig. 5*B*) and

macroscopic response (I_{max}) values (Fig. 5*C*) display a similar trend with an average periodicity of 3.3 amino acids for both of these functional parameters. These data suggest a helical secondary structure for γTM4.

The data presented in this study are consistent with a recently published secondary structure of the AChR (9), which proposes that all of the TM domains are helical. Using this model reveals that the only mutation that resulted in an increase in EC_{50}, L458W, faces the interior of the protein, specifically γTM1 (Fig. 6). A tryptophan replacement at this position may cause considerable steric hindrance, thus resulting in a mild increase in EC_{50}. Two of the mutations that resulted in increased nAChR expression and gain in function, L456W and F459W, face the lipid according to this model (Fig. 6). Similarly, A455W, which resulted in a remarkable gain in function and increased macroscopic and normalized macroscopic response, faces the lipid interface (Fig. 6). It is thus possible that the introduction of a lipophilic amino acid, such as tryptophan, in these lipid-exposed residues increases the efficiency of oligomerization and/or channel function.

The fact that expression and function of the AChR are not negatively affected by tryptophan replacements in γTM4 is consistent with the hypothesis that this domain is more loosely packed and/or has a wider crossing angle than the other AChR TM domains studied. To accommodate γTM4 in a wide crossing angle may require this TM domain to be more stretched along the lipid bilayer, thus resulting in a periodicity of less than 3.6. Our calculations yield average periodicity values of 3 amino acids for nAChR expression and 3.3 amino acids for nAChR function. The periodicity analysis presented here is consistent with the hypothesis that γTM4 has a wider crossing angle than the other subunits. Analysis of the model proposed by Miyazawa (9), however, does not reveal drastic differences in crossing angles for the TM domains within each subunit.

In summary, we have used tryptophan scanning mutagenesis to assess the role of γTM4 on the function of the AChR from *T. californica*. We have found that three mutations resulted in an increase in nAChR expression, whereas the others did not induce any change in nAChR expression relative to WT. A similar trend is apparent in the functional data, because four mutations resulted in an increase in function (decreased EC_{50} for ACh), whereas the others did not change in function relative to WT. The only exception for this was mutation L458W, which resulted in a modest increase in EC_{50}. These data suggest that this γTM4 is not as tightly packed as the other TM domains studied so far (*i.e.* αTM3, αTM4, and βTM3), because steric disruptions caused by the introduction of a large and lipophilic amino acid either do not affect or increase AChR oligomerization or function. Finally, the periodicity of changes, in both structure and function, suggest a helical secondary structure for the γTM4 of the *T. californica* AChR.

Acknowledgments—We especially thank Alexis Torres and Jose A. Lizardi for help with software-related problems. We also thank Dr. Manuel Navedo for help with the molecular modeling software and Dr. Madeline Nieves for help with computer hardware. We are grateful for the excellent technical help provided by Juan C. Galloza.

REFERENCES

1. Grutter, T., and Changeux, J. P. (2001) *Trends Biochem. Sci.* **26,** 459–463
2. Unwin, N. (1998) *J. Struct. Biol.* **121,** 181–190
3. Corringer, P. J., Le Novere, N., and Changeux, J. P. (2000) *Annu. Rev. Pharmacol. Toxicol.* **40,** 431–458
4. Karlin, A., and Akabas, M. H. (1995) *Neuron* **15,** 1231–1244
5. Hucho, F., Tsetlin, V. I., and Machold, J. (1996) *Eur. J. Biochem.* **239,** 539–557
6. Akabas, M. H., and Karlin, A. (1995) *Biochemistry* **34,** 12496–12500
7. Blanton, M. P., and Cohen, J. B. (1992) *Biochemistry* **31,** 3738–3750
8. Blanton, M. P., and Cohen, J. B. (1994) *Biochemistry* **33,** 2859–2872
9. Miyazawa, A., Fujiyoshi, Y., and Unwin, N. (2003) *Nature* **424,** 949–955
10. Methot, N., Demers, C. N., and Baenziger, J. E. (1995) *Biochemistry* **34,** 15142–15149
11. Baenziger, J. E., Morris, M. L., Darsaut, T. E., and Ryan, S. E. (2000) *J. Biol. Chem.* **275,** 777–784
12. Baenziger, J. E., and Methot, N. (1995) *J. Biol. Chem.* **270,** 29129–29137
13. Lugovskoy, A. A., Maslennikov, I. V., Utkin, Y. N., Tsetlin, V. I., Cohen, J. B., and Arseniev, A. S. (1998) *Eur. J. Biochem.* **255,** 455–461
14. Hasler, U., Crambert, G., Horisberger, J. D., and Geering, K. (2001) *J. Biol. Chem.* **276,** 16356–16364
15. Jenkins, A., Andreasen, A., Trudell, J. R., and Harrison, N. L. (2002) *Neuropharmacology* **43,** 669–678
16. Ueno, S., Lin, A., Nikolaeva, N., Trudell, J. R., Mihic, S. J., Harris, R. A., and Harrison, N. L. (2000) *Br. J. Pharmacol.* **131,** 296–302
17. Tamamizu, S., Guzman, G. R., Santiago, J., Rojas, L. V., McNamee, M. G., and Lasalde-Dominicci, J. A. (2000) *Biochemistry* **39,** 4666–4673
18. Tamamizu, S., Lee, Y., Hung, B., McNamee, M. G., and Lasalde-Dominicci, J. A. (1999) *J. Membr. Biol.* **170,** 157–164
19. Lee, Y. H., Li, L., Lasalde, J., Rojas, L., McNamee, M., Ortiz-Miranda, S. I., and Pappone, P. (1994) *Biophys. J.* **66,** 646–653
20. Lasalde, J. A., Tamamizu, S., Butler, D. H., Vibat, C. R., Hung, B., and McNamee, M. G. (1996) *Biochemistry* **35,** 14139–14148
21. Ortiz-Miranda, S. I., Lasalde, J. A., Pappone, P. A., and McNamee, M. G. (1997) *J. Membr. Biol.* **158,** 17–30
22. Bouzat, C., Gumilar, F., del Carmen Esandi, M., and Sine, S. M. (2002) *Biophys. J.* **82,** 1920–1929
23. Bouzat, C., Barrantes, F., and Sine, S. (2000) *J. Gen. Physiol.* **115,** 663–672
24. Bouzat, C., Roccamo, A. M., Garbus, I., and Barrantes, F. J. (1998) *Mol. Pharmacol.* **54,** 146–153
25. Cruz-Martin, A., Mercado, J. L., Rojas, L. V., McNamee, M. G., and Lasalde-Dominicci, J. A. (2001) *J. Membr. Biol.* **183,** 61–70
26. Guzman, G. R., Santiago, J., Ricardo, A., Marti-Arbona, R., Rojas, L. V., and Lasalde-Dominicci, J. A. (2003) *Biochemistry* **42,** 12243–12250
27. Santiago, J., Guzman, G. R., Torruellas, K., Rojas, L. V., and Lasalde-Dominicci, J. A. (2004) *Biochemistry* **43,** 10064–10070
28. Chothia, C. (1975) *Nature* **254,** 304–308
29. Noda, M., Takahashi, H., Tanabe, T., Toyosato, M., Kikyotani, S., Furutani, Y., Hirose, T., Takashima, H., Inayama, S., Miyata, T., and Numa, S. (1983) *Nature* **302,** 528–532
30. Claudio, T., Ballivet, M., Patrick, J., and Heinemann, S. (1983) *Proc. Natl. Acad. Sci. U. S. A.* **80,** 1111–1115
31. Methot, N., and Baenziger, J. E. (1998) *Biochemistry* **37,** 14815–14822
32. Unwin, N. (1993) *Cell* **72,** (suppl.) 31–41
33. Unwin, N. (1995) *Nature* **373,** 37–43
34. Unwin, N. (1993) *J. Mol. Biol.* **229,** 1101–1124
35. Sharp, L. L., Zhou, J., and Blair, D. F. (1995) *Proc. Natl. Acad. Sci. U. S. A.* **92,** 7946–7950
36. Sharp, L. L., Zhou, J., and Blair, D. F. (1995) *Biochemistry* **34,** 9166–9171

Protein Structure and Folding:

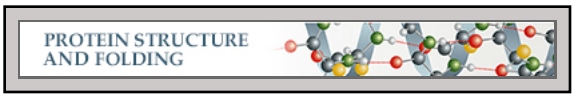

Tryptophan Scanning Mutagenesis of the γ M4 Transmembrane Domain of the Acetylcholine Receptor from *Torpedo californica*

Alejandro Ortiz-Acevedo, Mariel Melendez, Aloysha M. Asseo, Nilza Biaggi, Legier V. Rojas and José A. Lasalde-Dominicci

J. Biol. Chem. 2004, 279:42250-42257.
doi: 10.1074/jbc.M405132200 originally published online July 9, 2004
